Title

Early life energy expenditure deficits drive obesity in a mouse model of Alström syndrome

Authors

Erin J Stephenson[1,3,4], Clint E Kinney[1,3,5], Amanda S Statyton[1,3,6], Joan C Han[1,2,3,5]*

Affiliations

[1]Department of Pediatrics, College of Medicine, University of Tennessee Health Science Center, Memphis, TN, 38164, U.S.A.
[2]Department of Physiology, College of Medicine, University of Tennessee Health Science Center, Memphis, TN, 38164, U.S.A.
[3]Children's Foundation Research Institute, Le Bonheur Children's Hospital, Memphis, TN, 38104, U.S.A.
[4, #]Department of Anatomy, College of Graduate Studies and Chicago College of Osteopathic Medicine, Midwestern University, Downers Grove, IL 60515, U.S.A.
[5, #]Department of Pediatrics, Icahn School of Medicine at Mount Sinai and Kravis Children's Hospital, New York, NY, U.S.A.
[6, #]James D. Eason Transplant Institute, Department of Surgery, College of Medicine, University of Tennessee Health Science Center, Memphis, TN, 38164, U.S.A.
*Corresponding author, #Current affiliation

Abstract

Alström syndrome is an extremely rare multi-system disorder for which early-onset childhood obesity is one of the cardinal features. Similar to humans with Alström syndrome, animal models with *Alms1* loss of function mutations develop obesity, strongly supporting the notion that ALMS1/Alms1 is required for the regulatory control of energy balance across species. To determine which component(s) of energy balance are reliant on functional Alms1, we performed comprehensive energy balance phenotyping of the *tvrm*102 mouse model of Alström syndrome. We found that that adiposity gains occurred early and rapidly in male mice but much later in females. Rapid increases in body fat in males were, at least in part, due to a marked reduction in energy expenditure during early life and not due to any genotype-specific influence over energy intake. Energy intake did increase in a genotype-specific manner when mice were provided a palatable, high-energy diet, although this was not necessary for the initial establishment of obesity. Interestingly, the energy expenditure deficit observed in male *Alms1*-/- mice did not persist as mice age, suggesting that loss of Alms1 either causes a developmental delay in the mechanisms controlling early life energy expenditure, or that there is activation of compensatory mechanisms after obesity is established. Future studies will tease out how ALMS1/Alms1 modulates energy expenditure in early life and how sex moderates this process.

Key words

Alström syndrome, ALMS1, Primary cilia, Ciliopathy, Obesity, Adiposity, Metabolism, Energy balance, Energy Expenditure, Sex differences

Introduction

Primary cilia are non-motile membranous structures that protrude from the surface of all quiescent cells and many terminally differentiated cells [1]. They are dynamic organelles that act as cellular antennae that sense changes in the extracellular environment and communicate these changes to the cell [1, 2]. The localization and trafficking of receptors, ion channels and other proteins along the length of the primary cilium is essential for maintaining coordination of intracellular functions [1-4], and syndromes associated with defective cilia frequently manifest as a collection of metabolic defects and multi-organ dysfunction [5].

ALMS1 (Chr 2q13) encodes a 461 kDa protein located in the centrosomes and basal body of primary cilia [6, 7]. Although ALMS1 protein function is not completely understood [8, 9], humans with recessively inherited loss of function mutations in *ALSM1* manifest a ciliopathy known as Alström syndrome [8-10]. Alström syndrome is an extremely rare multi-system disorder characterized by early-onset childhood obesity, cone-rod retinal dystrophy, and sensorineural hearing loss [8-11]. Dilated cardiomyopathy, type-2 diabetes, and the progressive fibrosis and dysfunction of other organ systems (i.e., pulmonary, hepatic, and renal) are also frequently observed in these patients [8, 9, 11].

Mice with mutations in *Alms1* have normal ciliary formation [12, 13], but cilia progressively deteriorate over time, leading to a reduction in the total number of functional primary cilia with advancing age [13-15]. This phenomenon appears to occur randomly [15] and across multiple tissues [13-15], with especially rapid deterioration reported to occur in the hypothalamic region of the brain [13]. Similar to humans with Alström syndrome, mice [12, 13, 15-17] (and zebrafish [18]) with *Alms1* loss of function mutations develop obesity and hyperinsulinemia, strongly suggesting that ALMS1/Alms1 and long-term ciliary maintenance is required for effective regulatory control of energy balance.

Despite the observation that mice with *Alms1* loss of function mutations gain more body weight than their wild-type littermates [12, 15-17, 19-21], a comprehensive energy balance phenotype has not been established for any of the mouse models reported in the literature to date (Table 1). Increased adiposity [12, 15, 16, 20, 21] and increased food intake [16, 21] have been observed, and progressive hyperglycemia [12, 16, 20, 21] and hyperinsulinemia [12, 20] have also been reported. Since pair feeding only partially attenuates the obesity phenotype in *Alms1*-null mice [21], we hypothesized that obesity observed in Alms1 loss-of-function mutations may be driven, in part, via mechanisms of reduced energy expenditure. Here, we have characterized the energy balance phenotype of the Alms1^{Tvrm102} mouse model of Alström syndrome. We report sex-specific energy expenditure deficits in the absence of hyperphagia during the early stages of obesity development in *Alsm1* null mice.

Methods

Animals

Heterozygous *Alms1*^{tvrm102} mice were obtained from The Jackson Laboratory (C57BL/6J-Alms1$^{tvrm102/PjnMmjax}$, MMRRC Stock No: 43589-JAX). This strain originated as an ENU-induced T>C point mutation in the splice donor site of exon 6, which unmasks a cryptic splice site 120 bases downstream [19]. Experimental animals were generated by heterozygous cross and were genotyped using a custom Taqman SNP assay (Applied Biosystems #4332075, ANMFW9M). Only mice homozygous for the mutation (*Alms1*-/-) and their wild-type litter mates were studied (WT). Mice were housed at ~22°C in ventilated cages with cellulose bedding and free access to standard rodent chow (Envigo #7012) and an automated supply of filtered tap water. To determine whether food palatability influenced food intake, one cohort of mice were given free access to a palatable, high fat, sucrose-containing diet for two weeks (Research Diets #12451; 45% kCal from fat, 20% kCal from protein, 35% kCal from carbohydrate, including 17% from sucrose, 4.7 kCal/g), beginning at 15 weeks of age. In this cohort, food intake was measured daily for four weeks (one week of regular chow intake beginning at 14 weeks-of-age, two weeks of high fat diet intake, and another week of chow intake; Figure 4A).

Body composition, indirect calorimetry, activity, and food intake

From four weeks of age onwards, mice were weighed, and their body composition was measured by magnetic resonance (EchoMRI 1100) once per week (Figure 1A). Body length was determined as the distance from nose to the base of the tail in isoflurane-anesthetized mice at nine and 19-weeks of age. At eight or 18 weeks-of-age, chow-fed mice were individually housed in a high-resolution home cage-style Comprehensive Laboratory Animal Monitoring System (Columbus Instruments CLAMS-HC) set to simultaneously record respiratory gases via open-circuit indirect calorimetry, physical activity via infrared beam breaks, and food intake via load cell-linked hanging feeder baskets (Figure 1A). Water intake was measured by manually weighing water bottles. Energy expenditure and the respiratory exchange ratio were calculated from VO_2 and VCO_2 using the vendors software (Oxymax, Columbus Instruments), with the former determined using the Lusk equation [22]. Rates of fat and carbohydrate oxidation were calculated from VO_2 and VCO_2 data using previously reported equations [23] and the assumption that protein oxidation was negligible. Total physical activity was calculated as the combined number of beam breaks along both the X- and Y-axes, whereas ambulatory activity was calculated as the combined number of consecutive X- and Y-axes beam breaks occurring in a single series. The difference in beam breaks between ambulatory and total activity was considered the stereotypic activity (i.e., grooming, rearing and all other non-ambulatory movements). Food intake was determined from individual feeding bouts after which cumulative daily intake was calculated. Data for each mouse was collected over 7 days, at both ambient (22°C, 2-3 days) and thermoneutral housing conditions (28°C, 2-3 days). For each day of data collection, data were binned by hour and the hourly mean values (indirect calorimetry data) or summed values (activity and food intake data) over each 24-h measurement period were used

to determine the reported mean hourly values for each mouse. These data were analyzed using mixed linear models with total body weight, body fat and lean mass included as random effect variables (all parameters except RER), with non-normalized mean data ± standard error displayed in figures.

Statistics

Data are presented as the group means ± standard error unless otherwise stated. Longitudinal data were analyzed by mixed linear models with likelihood-ratio tests. All other data were assessed for homoscedasticity (Levene's test) and normality (Shapiro-Wilk test) before being compared using one of the following tests: normal data were analyzed using two-way ANOVA with Tukey post-hoc analysis; any multi-factorial non-normal data were analyzed using Scheirer-Ray-Hare tests with post hoc Wilcoxon Rank Sum tests adjusted for multiple comparisons using the Benjamini and Hochburg correction [24]. Pairwise comparisons were made using either Student's t-tests, Welch's t-tests or Wilcoxon Rank Sum tests. Data wrangling and analyses were performed in R Studio v1.2.5003 using R v3.6.1 and the statistical packages lme4 [25] (for linear models), car [26] (for Levene's tests), rcompanion [27] (for Scheirer-Ray-Hare tests). Differences between groups are discussed as significant where p-values are <0.05.

Results

Adiposity gains are observed early in male Alms1-/- mice but occur later in females

To characterize the development and progression of obesity following loss of Alms1 function, we established the body composition trajectory of both male and female *Alms1*-/- mice starting from four weeks of age (Figure 1B). Compared to their WT littermates, both male and female *Alms1*-/- mice progressively gain more adiposity as they age, with obesity occurring in male mice earlier and to a much greater magnitude than in female mice (Figure 1B). Specifically, compared to WT, male *Alms1*-/- mice had 20.4% more adiposity at five weeks of age (p=0.004) and had greater total body weight (6.9%, p=0.012) and greater lean mass by six weeks of age (6.3%, p=0.019). By 17 weeks of age, male *Alms1*-/- mice were 24.0% heavier (p<0.001) with 195.3% more body fat (p<0.001) and 5.8% more lean mass than their WT littermates (p=0.012). In contrast, *Alms1*-/- females had 7.7% less lean mass (p=0.035) and weighed 7.5% less (p=0.047) than their WT counterparts at five weeks of age. Increased adiposity was not observed in female *Alms1*-/- mice until 10 weeks of age (17.5%, p=0.009), whereas total body weight did not diverge from WT until 16 weeks of age (10.0%, p=0.021), at which point adiposity was 96.3% greater in *Alms1*-/- females compared to WT (p<0.001). By 17 weeks of age, female *Alms1*-/- mice were 11.9% heavier than WT, with 119.7% greater adiposity that their WT littermates (p<0.001). We no longer observed differences in lean mass between the two genotypes in females at 17 weeks of age. Although an effect of age was observed for the body length of both male and female mice (p<0.001 and p=0.01, respectively), differences in body composition were not driven by genotype-associated

differences in body length in male mice (p=0.903), whereas there was tendency for genotype to influence the body length of female mice (p=0.052; Figure 1C), with WT females growing 4% longer between nine and nineteen weeks-of-age (p=0.022) during which time the length of *Alms1*-/- females remained reasonably stable (0.07%, p=0.978).

Both sexes are less active but only male Alms1-/- mice have lower total energy expenditure

To identify which determinants of energy balance might be contributing to the increased adiposity we observed in *Alms1*-/- mice, we performed indirect calorimetry experiments while simultaneously measuring physical activity and food intake (Figures 1A, 2, and 3). We initially performed these experiments in eight-week-old mice to limit the confounding influence of the marked divergence in bodyweight observed in older mice. Under ambient temperature housing conditions (22°C, Figure 2A), we observed that compared to WT, 8-week-old male *Alms1-/-* mice had distinctly lower 24-hour energy expenditure (Figure 2A, upper panel, left; p=0.008), a finding consistent across both the photophase (p=0.017) and scotophase (p=0.005) photoperiods. Lower energy expenditure was due, in part, to *Alms1*-/- mice having reduced 24-hour ambulatory activity (Figure 2A, second panel, left; p=0.014), primarily driven by differences in activity during the scotophase (p=0.010). No differences in stereotypic activity were observed between genotypes (Supplementary Figure 1A, left panel). In contrast, the 24-hour energy expenditure of female mice was not different between genotypes (Figure 2A, upper panel, right; p=0.511). Due to photophase ambulatory activity being lower in female *Alms1*-/- mice (Figure 2A, second panel, right; p=0.009), there was a tendency for 24-hour ambulatory activity to be lower in *Alms1*-/- females compared to WT (p=0.055), although this was not significant. Similar to our findings in males, no differences in stereotypic activity were observed between genotypes in female mice (Supplementary Figure 1A, right panel).

Alms1-/- mice eat similarly to WT but have altered substrate oxidation

In male mice, neither cumulative or total 24-hour food intake differed between the genotypes (Figure 2A, center panel; p=0.096 and p=0.872, respectively); however, noticeable differences in substrate oxidation were observed. Specifically, rates of 24-hour lipid oxidation were suppressed in male *Alms1*-/- mice compared to WT (Figure 2A, fourth panel, left; p=0.029), an observation primarily driven by lower rates of lipid oxidation during the photophase (p=0.004). Similarly, rates of 24-hour carbohydrate oxidation were reduced in male *Alms1*-/- mice compared to WT (Figure 2A, lower panel, left; p=0.009); this observation was primarily driven by lower rates of carbohydrate oxidation throughout the scotophase (p=0.003). Differences in substrate oxidation were reflected in the RER values, with male *Alms1-/-* mice having a lower scotophase RER than WT (Supplementary Figure 1B, left panel, p=0.045). Similar to our observations in male mice, female mice did not differ with respect to genotype when it came to cumulative or total 24-hour food intake (Figure 2A, center panel, right; p=0.743 and p=0.665). However,

differences in substrate oxidation were observed. Female *Alms1-/-* mice had higher rates of scotophase lipid oxidation compared to WT (Figure 2A, fourth panel, right; p=0.047), despite overall 24-hour lipid oxidation being similar to WT. Rates of carbohydrate oxidation were similar between genotypes for female mice (Figure 2A, lower panel, right; p=0.630). Higher rates of scotophase lipid oxidation were reflected as reduced scotophase and 24-hour RER values (p=0.014 and p=0.049, respectively, Supplementary Figure 1B, right panel).

Deficits in energy expenditure and substrate oxidation persist in male Alms1-/- mice when housed under thermoneutral conditions

To ensure any differences (or lack-there-of) we observed were not a consequence of thermal stress caused by housing mice at temperatures considered ambient for humans but cold for mice, enclosure temperatures were increased to within the murine thermoneutral zone (28°C) after which mice were monitored for an additional 2-3 days (Figures 1A and 2B). We found that the lower energy expenditure we observed in male *Alms1*-/- mice under ambient conditions persisted during both photoperiods when housed under thermoneutral conditions (Figure 2B, upper panel, left; photophase: p=0.007, scotophase: p=0.007, and 24-hours: p=0.003), a finding consistent with *Alms1*-/- males maintaining reduced levels of ambulatory activity compared to WT (Figure 2B, second panel, left; photophase: p=0.015, scotophase: p=0.006, and 24-hours: p=0.004). Also in line with our findings at ambient temperature, female *Alms1*-/- and WT mice displayed similar energy expenditures (Figure 2B, upper panel, right), despite *Alms1*-/- females being less active than WT during the photophase photoperiod (Figure 2B, second panel, right; p=0.015). Genotype had no effect on stereotypic activity in either sex under thermoneutral housing conditions (Supplementary Figure 1C).

Both cumulative and total 24-hour food intake remained similar between the genotypes for male mice housed under thermoneutral conditions (Figure 2B, center panel, left; p= 0.636 and p=0.684, respectively); however, female *Alms1*-/- mice had slightly elevated cumulative intake (Figure 2B, center panel, right; p=0.045), driven by differences at the end of the photophase photoperiod (p=0.010), although this did not translate to more food eaten after 24 h, as no difference in total 24 h intake was observed between the two genotypes (p=0.653). Lipid oxidation remained lower in *Alms1*-/- males compared to WT (Figure 2B, fourth panel, right; photophase: p=0.008, scotophase: p=0.042, and 24-hours: p=0.007), as did carbohydrate oxidation (p=0.026), although this was primarily driven by differences during the photophase (Figure 2B, lower panel, left; p=0.011). Rates of lipid and carbohydrate oxidation were similar between female *Alms1*-/- and WT mice when housed under thermoneutral conditions (Figure 2B, lower two panels, right; p=0.252 and p=0.590, respectively).

Aging attenuates the energy expenditure deficits observed in younger male Alms1-/- mice

Since differences body composition did not manifest in female *Alms1-/-* mice until a later stage and no deficit in energy expenditure was observed in 8-week old females (whereas both body composition and energy expenditure were both different in young *Alms1-/-* males compared to WT), we repeated indirect calorimetry experiments in a cohort of older mice to determine if females might acquire a similar energy balance phenotype to male mice as they age (Figure 1A and Figure 3). Similar to our findings in younger mice, 24-hour energy expenditure was not different in *Alms1-/-* females compared to WT (Figure 3A, upper panel, right; p=0.899) despite *Alms1-/-* females having increased adiposity by this age (Figure 1B). Differences in ambulatory activity observed in younger females were not present in older mice, with both ambulatory and stereotypic activity being similar in *Alms1-/-* mice compared to WT (Figure 3A, second panel, right; p=0.263, and Supplementary Figure 2A; p=0.298). Neither cumulative (p=0.747) or 24-hour food intake differed between the genotypes in females, whereas lipid (p=0.951) or carbohydrate oxidation (p=0.987) were also not different when body composition was considered (Figure 3A, lower two panels). In contrast to our observations in younger male mice, 24-hour energy expenditure in older *Alms1-/-* males was not different to WT (Figure 3A upper panel, left; p=0.869). Activity differences present in younger mice were also no longer present in older male mice (Figure 3A, second panel, left; p=0.888). No differences in food intake were observed, although there was a tendency for cumulative intake in male *Alms1-/-* to be less than WT (Figure 3A, left, center panel; p=0.096). Similar to older females, no differences in lipid (p=0.952) or carbohydrate oxidation (p=0.854) were detected after considering body composition in the comparison (Figure 3A, let, lower two panels). Similar observations were made for all parameters in both sexes when older mice were housed under thermoneutral conditions (Figure 3B); the only exception being that there was a tendency for male *Alms1*-/- mice to have increased carbohydrate oxidation compared to WT when thermal stress was reduced (Figure 3B, last panel, left; p=0.052).

Alms1-/- mice eat more than wild-type mice when provided a palatable high fat diet

Two previous studies have reported that both male and female *Alms1*-/- (*foz/foz*) mice consume more food than their wild-type littermates [16, 21]; however, we were unable to replicate this observation in either the younger or older *Alms1*-/- mice in our own chow-fed cohorts. To address this discrepancy, we sought to determine whether food palatability influenced food intake in a separate cohort of *Alms1*-/- mice (Figure 4). Mice were given a week to acclimate to being housed individually, after which chow intake was measured daily for one week. Food was then switched from chow to a palatable high-fat diet for two weeks, and then back to chow for a final week. In addition to recording daily food intake over the four-week period, we also measured body composition on a weekly basis (Figure 4A).

In line with our earlier findings, compared to wild-type, *Alms1*-/- males (and one *Alms1*-/- female) had increased adiposity while consuming a standard chow diet (Figure 4B), yet did not consume any more food than wild-type littermates (Figure 4C). During the high-fat diet phase, both wild-type and *Alms1*-/-

mice gained body weight and increased their adiposity (Figure 4B); however, these gains were exacerbated in the *Alms1*-/- cohort (Figure 4B, upper panel, p=0.007, and center panel, p=0.001). Increases in body weight and adiposity in *Alms1*-/- mice appeared to be due to greater caloric intake compared to wild-type mice during this period (Figure 4C, p<0.001). Both wild-type and *Alms1*-/- mice lost weight and adiposity upon withdrawal of the high-fat diet and a return to chow (Figure 4B), an observation associated with a reduction in energy intake due to the change in diets. No differences in energy intake were detected between the genotypes after the diet was switched back to chow (Figure 4C). These data suggest that in the *tvrm102* mouse model of Alström syndrome, increased energy intake only occurs in the setting of a palatable, high-energy diet.

Discussion

Here, we have performed comprehensive energy balance phenotyping of a mouse model of Alström syndrome. The data we present demonstrate that in the *tvrm102* mouse model of Alström syndrome, adiposity gains occur early and rapidly in male mice, but occur much later in females. Rapid increases in body fat in males are, at least in part, due to a marked reduction in energy expenditure during early life and not due to any genotype-specific influence over energy intake. Energy intake does increase in a genotype-specific manner when mice are provided a palatable, high-energy diet, although this is not necessary for the initial establishment of obesity. Interestingly, the energy expenditure deficit observed in male *Alms1*-/- mice does not persist as mice age, suggesting that loss of *Alms1* either causes a developmental delay in the mechanisms controlling early life energy expenditure, or that there is activation of compensatory mechanisms after obesity is established. Teasing out how ALMS1 modulates energy expenditure in early life and how sex moderates this process will be a key step in understanding how mutations in ALMS1 lead to childhood obesity in Alström syndrome.

One of the cardinal features of Alström syndrome is the rapid onset of obesity during early childhood [28]. Reports indicate that the average body fat of individuals diagnosed with Alström syndrome ranges from 34.7-38.4% [11, 29], with male patients thought to gain proportionally more body fat than females [29]. However, since patient cohort data are typically not separated by sex due to Alström syndrome's ultra-rare incidence [30], it has been challenging to parse out whether sex does indeed moderate the progression of obesity in these patients. Mouse models of Alström syndrome should be able to fill this gap in our understanding, although to date, body composition data collected for either sex has primarily been limited to single (or random) timepoints that make it difficult to infer anything about obesity onset and its progression over time [12, 15, 16]. Here, we provide new insight into the timing of obesity onset and rate of obesity progression, demonstrating that *Alms1*-/- male mice become obese earlier and gain adiposity more rapidly than females, supporting the preliminary observation that male patients with Alström syndrome may gain more absolute body fat than female patients [29].

It has been suggested that patients with Alström syndrome develop obesity as a result of increased caloric intake as opposed to a deficit in resting energy expenditure [11]; however, data are inconclusive on whether loss of ALMS1 function drives hyperphagia or if other determinants of energy balance also contribute to obesity in these patients [31]. Caregiver hyperphagia questionnaire scores from one patient cohort suggest that hyperphagia may be elevated in people with Alström syndrome compared to age-, sex-, race-, and BMI Z-score-matched control subjects [11], and short-term food intake measurements in the *foz/foz* mouse model support this notion [16]. But besides these reports, limited data exist – in either animal models or patients – to support the assertion that obesity in Alström syndrome is driven solely by overeating. To address this issue and strengthen our understanding of how mutations in *ALMS1*/*Alms1* disrupt energy balance to cause obesity, we performed comprehensive energy balance phenotyping in both younger (8-week-old) and older (18-week-old) adult mice. Energy expenditure was determined in home cages while simultaneously measuring food intake and physical activity so that we could get a complete picture of how Alms1 influences the key physiologic mechanisms that determine energy balance. Unlike previous studies that have suggested loss of Alms1 function results in hyperphagia [16, 21], we did not observe any differences in food intake in *Alms1-/-* mice compared to wild-type mice. If anything, older male *Alms1*-/- mice had a tendency to eat less when provided a standard laboratory chow diet. We did, however, find that when provided a high-energy, palatable diet, both male and female *Alms1*-/- mice ate more than wild-type mice, an effect that was completely reversed after returning the mice to a chow diet. This observation, together with the finding that pair-feeding *foz/foz* males (high-fat diet matched to wild-type intake) does not prevent weight gain but does ameliorate some of the other metabolic consequences of Alms1 loss-of-function [21], suggests that although some combination of food environment and an altered hedonic response to food might exacerbate obesity in *Alms1*-/- mice, it is not the primary driving factor.

Our observation that younger male mice have markedly reduced energy expenditure compared to their wild-type littermates further supports the notion that altered thermogenic capacity at an early age, rather than overeating, drives the obesity phenotype of *Alms1*-/- mice. In line with this, it has been reported that *foz/foz* males have comparable normalized VO_2 (reported as VO_2 per unit body mass scaled to 2/3) when receiving a chow diet, but fail to increase their oxygen consumption by the same magnitude as wild-type mice when consuming a high fat diet [21]. This suggests that *foz/foz* mice likely have a defect in the mechanisms controlling the non-resting thermogenic pathways. Indeed, it has been shown that *foz/foz* mice are unable to maintain their core body temperature when subjected to acute cold exposure, in part because of an attenuated induction of thermogenic transcripts and a reduced capacity for glucose uptake into brown adipose tissue [21]. Interestingly, repeated cold exposure (2 h/d at 4°C for 4 weeks) corrects the ability of high fat diet fed *foz/foz* mice to maintain core temperature during a cold challenge, while also restoring the thermogenic profile of adipose tissues and limiting high fat diet

induced weight gain [21]. These observations suggest that although *Alms1* influences the energetic response to acute thermogenic challenges, some of the deleterious effects caused by loss of Alms1 function can be overcome by 'training' the thermogenic pathways to respond. In our study, reduced energy expenditure in male *Alms1*-/- mice could be explained in part by younger mice being less active. Given the adaptability of cold tolerance previously observed in the *foz/foz* mouse strain [21], it is plausible that increasing activity through regular exercise training may also help overcome the early life energy expenditure deficits in male *Alms1*-/- mice. To date, few studies have attempted to quantified activity levels in *Alms1*-/- mouse models, and no reports of activity levels in patients with Alström syndrome are available. Given that resting energy expenditure no longer appears to be different between patients with Alström syndrome and age-, sex-, race-, and BMI Z-score-matched control subjects after adjusting for differences in lean body mass [11], understanding how ALMS1 affects adaptive thermogenic pathways (exercise, NEAT, thermic effect of food, etc.) will be an important next line of investigation that may open the door to new therapeutics aimed at increasing energy expenditure and attenuation of weight gain.

Curiously, adiposity has been found to lessen after patients with Alström syndrome reach adulthood; however, the cause of this progressive reversal is debated [28, 30]. One suggestion is that the attenuation of obesity coincides with the onset or increased severity of other clinical complications [12], whereas others disagree and have instead postulated that weight loss in adults may be due to lifestyle modifications made after diabetes onset [28], or that adipose tissue becomes metabolically inflexible and a type of lipodystrophy develops [31]. In this study we did not follow the mice long enough to observe attenuation of adiposity gains as the mice aged; however, we can speculate that our observation of age-associated reversal of the energy expenditure deficit seen in younger male mice may contribute to this phenomenon. Increased energy expenditure without a change in energy intake would be expected to lead to weight loss or slowing of weight gain over time and may partially explain the attenuation in adiposity observed in patients with Alström syndrome after they reach adulthood. How or why energy expenditure deficits reverse over time in *Alms1*-/- mice and whether this phenomenon also occurs in patients with Alström syndrome are important questions that future studies should aim to address.

Conclusion

The data we present strengthen our understanding of the role of ALMS1/Alms1 in energy balance regulation. Using the *tvrm102* mouse model of Alström syndrome, we demonstrate that *Alms1* mutations cause early and rapid adiposity gains in male mice, with adiposity gains occurring much later in females. Rapid increases in body fat in males are, at least in part, due to a marked reduction in early life energy expenditure and not due to any genotype-specific influence over energy intake. Increased energy intake

does occur with exposure to a palatable, high-energy diet, but this is not necessary for obesity to progress in these mice. If we were to extrapolate these findings to patients with Alström syndrome, this suggests that biological sex and food environment are major determinants of the rate at which obesity manifests and its overall severity. Whether deficits in early life energy expenditure can be targeted to attenuate obesity severity in Alström syndrome is an important question that future studies should address.

References

1. Walz, G., *Role of primary cilia in non-dividing and post-mitotic cells.* Cell Tissue Res, 2017. **369**(1): p. 11-25.
2. Anvarian, Z., et al., *Cellular signalling by primary cilia in development, organ function and disease.* Nat Rev Nephrol, 2019. **15**(4): p. 199-219.
3. Long, H. and K. Huang, *Transport of Ciliary Membrane Proteins.* Front Cell Dev Biol, 2019. **7**: p. 381.
4. Nachury, M.V. and D.U. Mick, *Establishing and regulating the composition of cilia for signal transduction.* Nat Rev Mol Cell Biol, 2019. **20**(7): p. 389-405.
5. Hildebrandt, F., T. Benzing, and N. Katsanis, *Ciliopathies.* N Engl J Med, 2011. **364**(16): p. 1533-43.
6. Collin, G.B., et al., *Mutations in ALMS1 cause obesity, type 2 diabetes and neurosensory degeneration in Alstrom syndrome.* Nat Genet, 2002. **31**(1): p. 74-8.
7. Hearn, T., et al., *Mutation of ALMS1, a large gene with a tandem repeat encoding 47 amino acids, causes Alstrom syndrome.* Nat Genet, 2002. **31**(1): p. 79-83.
8. Hearn, T., *ALMS1 and Alstrom syndrome: a recessive form of metabolic, neurosensory and cardiac deficits.* J Mol Med (Berl), 2019. **97**(1): p. 1-17.
9. Marshall, J.D., et al., *Alstrom syndrome.* Eur J Hum Genet, 2007. **15**(12): p. 1193-202.
10. Alstrom, C.H., et al., *Retinal degeneration combined with obesity, diabetes mellitus and neurogenous deafness: a specific syndrome (not hitherto described) distinct from the Laurence-Moon-Bardet-Biedl syndrome: a clinical, endocrinological and genetic examination based on a large pedigree.* Acta Psychiatr Neurol Scand Suppl, 1959. **129**: p. 1-35.
11. Han, J.C., et al., *Comprehensive Endocrine-Metabolic Evaluation of Patients With Alstrom Syndrome Compared With BMI-Matched Controls.* J Clin Endocrinol Metab, 2018. **103**(7): p. 2707-2719.
12. Collin, G.B., et al., *Alms1-disrupted mice recapitulate human Alstrom syndrome.* Hum Mol Genet, 2005. **14**(16): p. 2323-33.
13. Heydet, D., et al., *A truncating mutation of Alms1 reduces the number of hypothalamic neuronal cilia in obese mice.* Dev Neurobiol, 2013. **73**(1): p. 1-13.
14. Jagger, D., et al., *Alstrom Syndrome protein ALMS1 localizes to basal bodies of cochlear hair cells and regulates cilium-dependent planar cell polarity.* Hum Mol Genet, 2011. **20**(3): p. 466-81.
15. Li, G., et al., *A role for Alstrom syndrome protein, alms1, in kidney ciliogenesis and cellular quiescence.* PLoS Genet, 2007. **3**(1): p. e8.
16. Arsov, T., et al., *Fat aussie--a new Alstrom syndrome mouse showing a critical role for ALMS1 in obesity, diabetes, and spermatogenesis.* Mol Endocrinol, 2006. **20**(7): p. 1610-22.
17. Geberhiwot, T., et al., *Relative Adipose Tissue Failure in Alstrom Syndrome Drives Obesity-Induced Insulin Resistance.* Diabetes, 2021. **70**(2): p. 364-376.
18. Nesmith, J.E., et al., *Genomic knockout of alms1 in zebrafish recapitulates Alstrom syndrome and provides insight into metabolic phenotypes.* Hum Mol Genet, 2019. **28**(13): p. 2212-2223.
19. Krebs, M.P., et al., *Mouse models of human ocular disease for translational research.* PLoS One, 2017. **12**(8): p. e0183837.
20. Favaretto, F., et al., *GLUT4 defects in adipose tissue are early signs of metabolic alterations in Alms1GT/GT, a mouse model for obesity and insulin resistance.* PLoS One, 2014. **9**(10): p. e109540.

21. Poekes, L., et al., *Defective adaptive thermogenesis contributes to metabolic syndrome and liver steatosis in obese mice.* Clin Sci (Lond), 2017. **131**(4): p. 285-296.
22. Lusk, G., *Animal Calorimetry: Twenty-Fourth Paper. Analysis of the Oxidation of Mixtures of Carbohydrate and Fat.* Journal of Biologial Chemistry, 1924. **59**: p. 41-42.
23. Peronnet, F. and D. Massicotte, *Table of nonprotein respiratory quotient: an update.* Can J Sport Sci, 1991. **16**(1): p. 23-9.
24. Benjamini Y, H.Y., *Controlling the false discovery rate: a practical and powerful approach to multiple testing.* J R Stat Soc Ser B Methodol, 1995. **57**: p. 289-300.
25. Bates D, M.M., Bolker B, Walker S, *Fitting Linear Mixed-Effects Models Using lme4.* Journal of Statistical Software, 2015. **67**(1): p. 1–48.
26. Fox J, W.S., *An R Companion to Applied Regression, Third edition.* . 3 ed. 2019, Thousand Oaks CA: Sage,.
27. Mangiafico, S.S., *Summary and Analysis of Extension Program Evaluation in R*. Vol. version 1.18.1. 2016.
28. Marshall, J.D., et al., *Alstrom syndrome: genetics and clinical overview.* Curr Genomics, 2011. **12**(3): p. 225-35.
29. Minton, J.A., et al., *Syndromic obesity and diabetes: changes in body composition with age and mutation analysis of ALMS1 in 12 United Kingdom kindreds with Alstrom syndrome.* J Clin Endocrinol Metab, 2006. **91**(8): p. 3110-6.
30. Tahani, N., et al., *Consensus clinical management guidelines for Alstrom syndrome.* Orphanet J Rare Dis, 2020. **15**(1): p. 253.
31. Marshall, J.D., et al., *New Alstrom syndrome phenotypes based on the evaluation of 182 cases.* Arch Intern Med, 2005. **165**(6): p. 675-83.

Conflict of interest statements

J.C.H. is a site-PI for a multicenter clinical trial sponsored by Rhythm Pharmaceuticals. The remaining authors have no conflict of interest to declare.

Author contributions

E.J.S. and J.C.H. designed the study. E.J.S., A.S.S. and C.E.K. performed the experiments. E.J.S. analyzed the data and prepared the manuscript. J.C.H. provided feedback on the initial draft of the manuscript and all authors approved the submitted version of the manuscript.

Funding

This study was supported by the Memphis Research Consortium and the Le Bonheur Children's Foundation Research Center.

Tables

Table 1: Overview of mouse models with systemic *Alms1* mutations and their metabolic abnormalities

Model	Mutation	Background	Metabolic observations compared to wild-type littermates	Citation(s)
foz/foz fed a chow diet	Spontaneous 11 bp deletion in exon 8 causing a frameshift mutation that generates a premature stop codon	NOD (Non Obese Diabetic)	• ↑ Body mass index • ↑ Adiposity • ↑ Lean body mass • ↑ Body length (females only) • ↑ Daily food intake • Hepatic steatosis • Hyperinsulinemia • Hyperglycemia • ↓ Glucose tolerance	[16, 21]

			• Enlarged pancreatic islets • ↑ Serum cholesterol (total) • ↔ $BW^{0.66}$ normalized VO_2 (males) • ↔ Habitual physical activity (males)	
foz/foz fed a high-fat diet (males only)	Spontaneous 11 bp deletion in exon 8 causing a frameshift mutation that generates a premature stop codon	NOD (Non Obese Diabetic)	• > ↑ Body weight • > ↑ Adiposity • > ↑ Adipocyte hypertrophy • > ↑ Daily food intake • Hepatic steatosis • Hyperglycemia • ↓ Glucose tolerance • ↓ Insulin responsiveness • ↔ Body temperature • ↓ $BW^{0.66}$ normalized VO_2 • ↔ Habitual physical activity	[21]
Gt(XH152)	Gene trap – intron 13	C57BL6/J x 129P2Ola	• ↑ Body weight • ↑ Adiposity • Adipocyte hypertrophy • Hepatic steatosis • Hyperinsulinemia • Hyperglycemia • ↓ Glucose tolerance • Enlarged pancreatic islets • ↑ Serum leptin • ↑ Serum cholesterol (total) • ↑ Serum ALT (late) • ↔ Serum triglycerides	[12, 20]
L2131X/L2131X	ENU-generated nonsense mutation in exon 10 TTA>TAA that generates a premature stop codon	C57BL6/J x NOD	• ↑ Body weight • ↑ Adiposity • Adipocyte hypertrophy • Hepatic steatosis • Hyperinsulinemia • Euglycemia • ↑ Serum leptin • ↑ Serum cholesterol (total & HDL) • ↑ Serum triglycerides	[15]
tvrm102	ENU-generated splice mutation in exon 6 T>C generating a premature stop codon	C57BL6/J	• ↑ Body weight	[19]
flin/flin (3-month-old males)	Frt-lacZ-LoxP-Neo-Frt-LoxP sequence inserted between exon 6 and exon 7	C57BL6/N	• ↑ Body weight • Adipocyte hypertrophy • ↓ Glucose tolerance • ↓ Insulin responsiveness • Metabolic defects corrected with Adipoq-Cre driven *Alms1* reactivation	[17]

Figure legends

Figure 1: Body weight gains in *Alms1*-/- mice are caused by increases in adiposity from an early age
A. Overview of experimental design. B. Body composition of *Alms1*-/- and wild-type male (n=25-16 and n=21-24, respectively) and female mice (n=11-15 and n=19-22, respectively) from 4 weeks of age onward. C. Body length of *Alms1*-/- and wild-type male and female mice at 9- and 19 weeks-of-age. Values displayed are mean ± se. Open circles/bars denote wild-type, closed circles/bars denote *Alms1*-/-. *p<0.05

Figure 2: Energy balance phenotype of *Alms1*-/- and wild-type mice between 8-9 weeks-of-age
A. Daily energy expenditure, ambulatory activity, cumulative food intake, lipid oxidation, and carbohydrate oxidation measured at 22°C, and B. 28°C in *Alms1*-/- and wild-type male (n=8 and n=11, respectively) and female mice (n=5 and n=9, respectively). Data presented are group means ± se. Open circles denote wild-type, closed circles denote *Alms1*-/-. Grey shading denotes scotophase photoperiod. For each photoperiod, p-values were generated from likelihood-ratio tests comparing mixed linear models for each parameter (note: body weight, body fat, and lean mass were included as random factors in the models).

Figure 3: Energy balance phenotype of *Alms1*-/- and wild-type mice between 18-19 weeks-of-age
A. Daily energy expenditure, ambulatory activity, cumulative food intake, lipid oxidation, and carbohydrate oxidation measured at 22°C, and B. 28°C in *Alms1*-/- and wild-type male (n=8 and n=11, respectively) and female mice (n=10 and n=17, respectively). Data presented are group means ± se. Open circles denote wild-type, closed circles denote *Alms1*-/-. Grey shading denotes scotophase photoperiod. For each photoperiod, p-values were generated from likelihood-ratio tests comparing mixed linear models for each parameter (note: body weight, body fat, and lean mass were included as random factors in the models).

Figure 4: *Alms1*-/- mice eat more than wild-type mice when provided a palatable high fat diet
A. Overview of experimental design. B. Body composition of *Alms1*-/- and wild-type male (n=3 and n=4-5, respectively) and female mice (n=1 and n=1, respectively) before, during, and after a two-week period of high-fat feeding. C. Energy intake of *Alms1*-/- and wild-type male (n=3 and n=4-5, respectively) and female mice (n=1 and n=1, respectively) before, during, and after a two-week period of high-fat feeding. Data presented are group means ± se (except for females where n=1/group). Open circles denote wild-type, closed circles denote *Alms1*-/-. Grey shading denotes high-fat diet phase. For the high-fat diet phase, linear models were compared using likelihood-ratio tests and these p-values are reported on the figures.

A

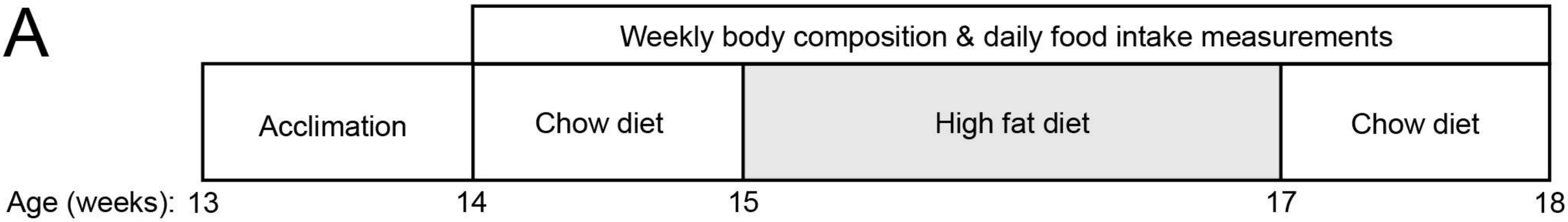

B

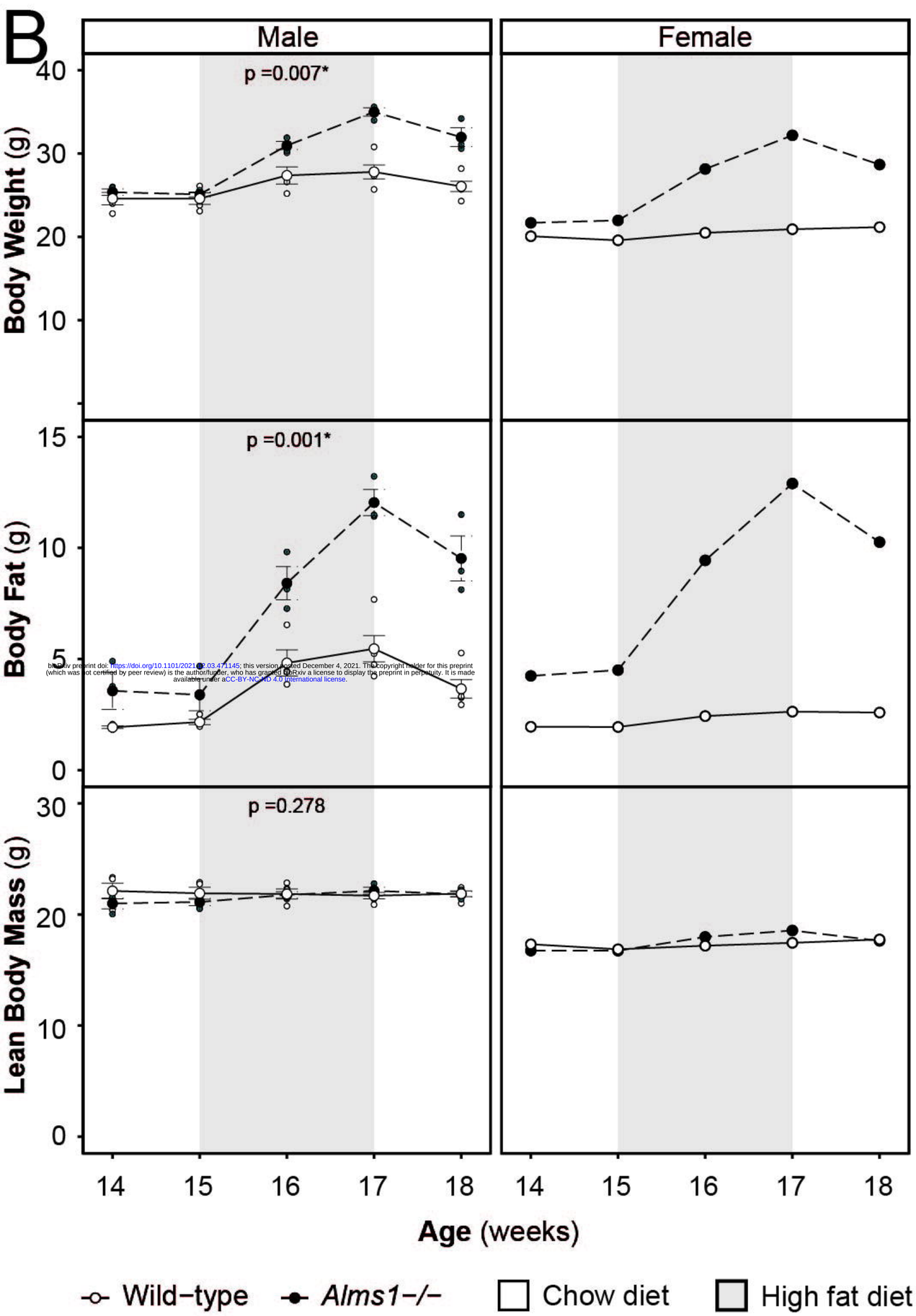

C

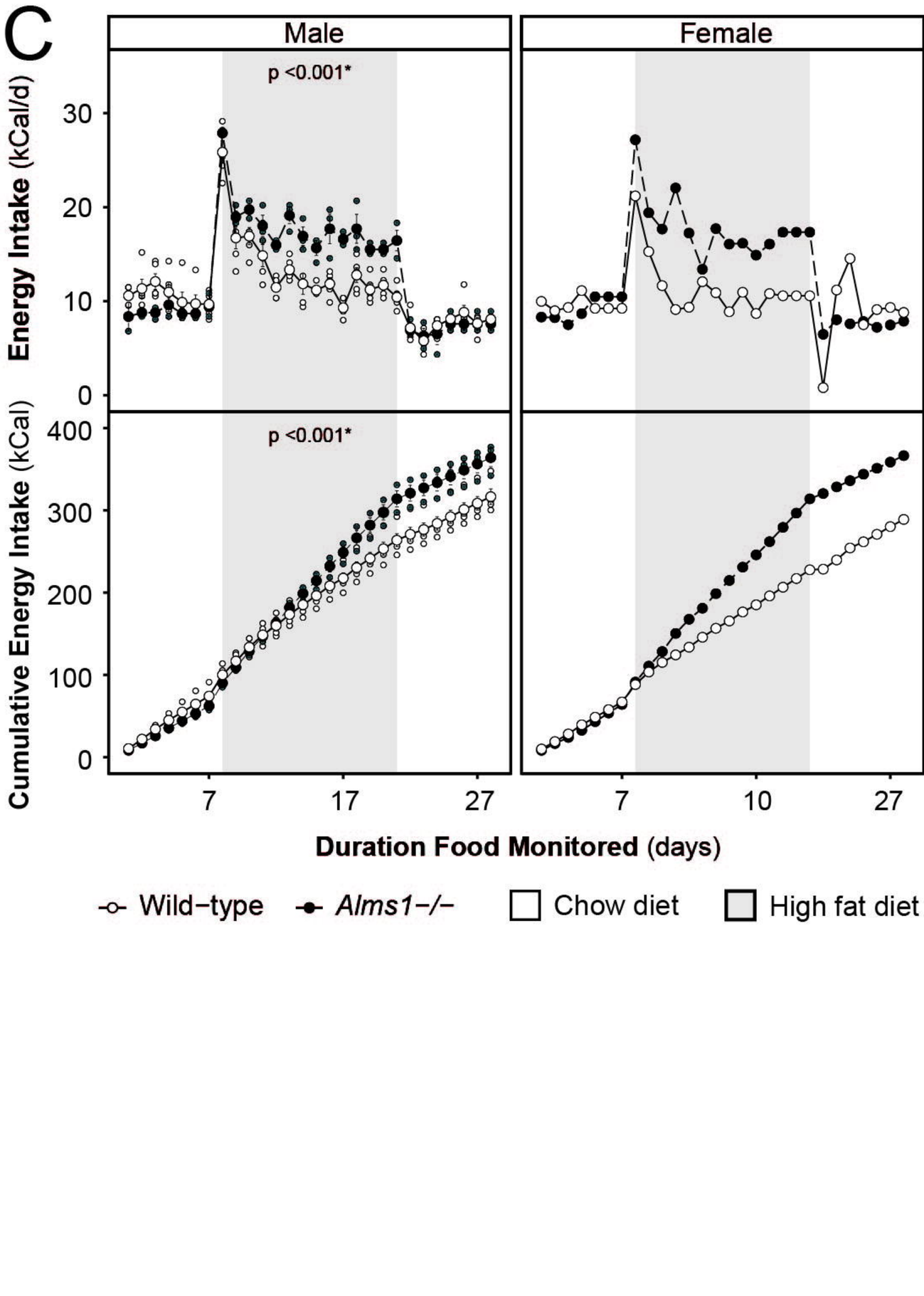

A

Ambient temperature housing

Thermoneutral zone housing (28˚C)

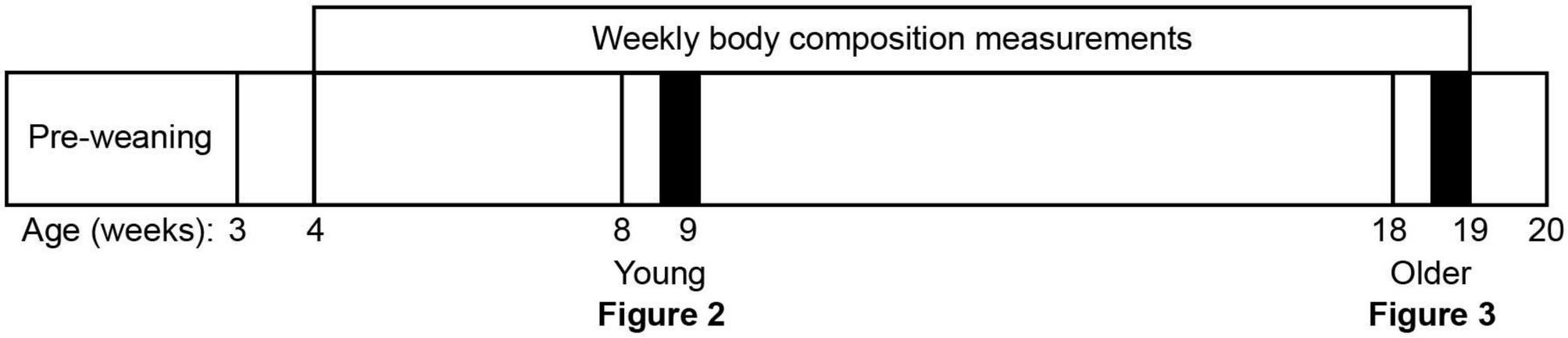

Figure 2 **Figure 3**

B

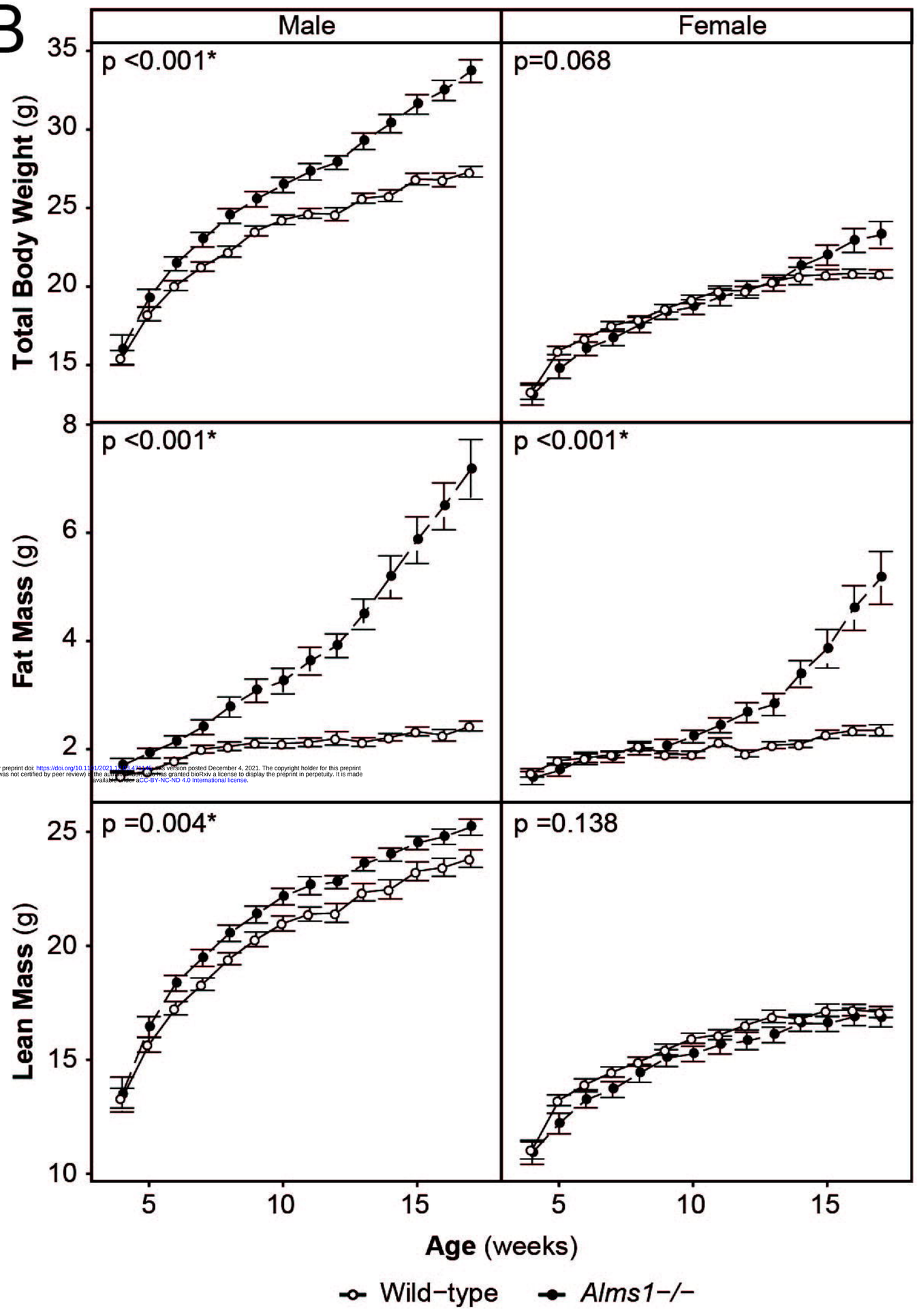

C